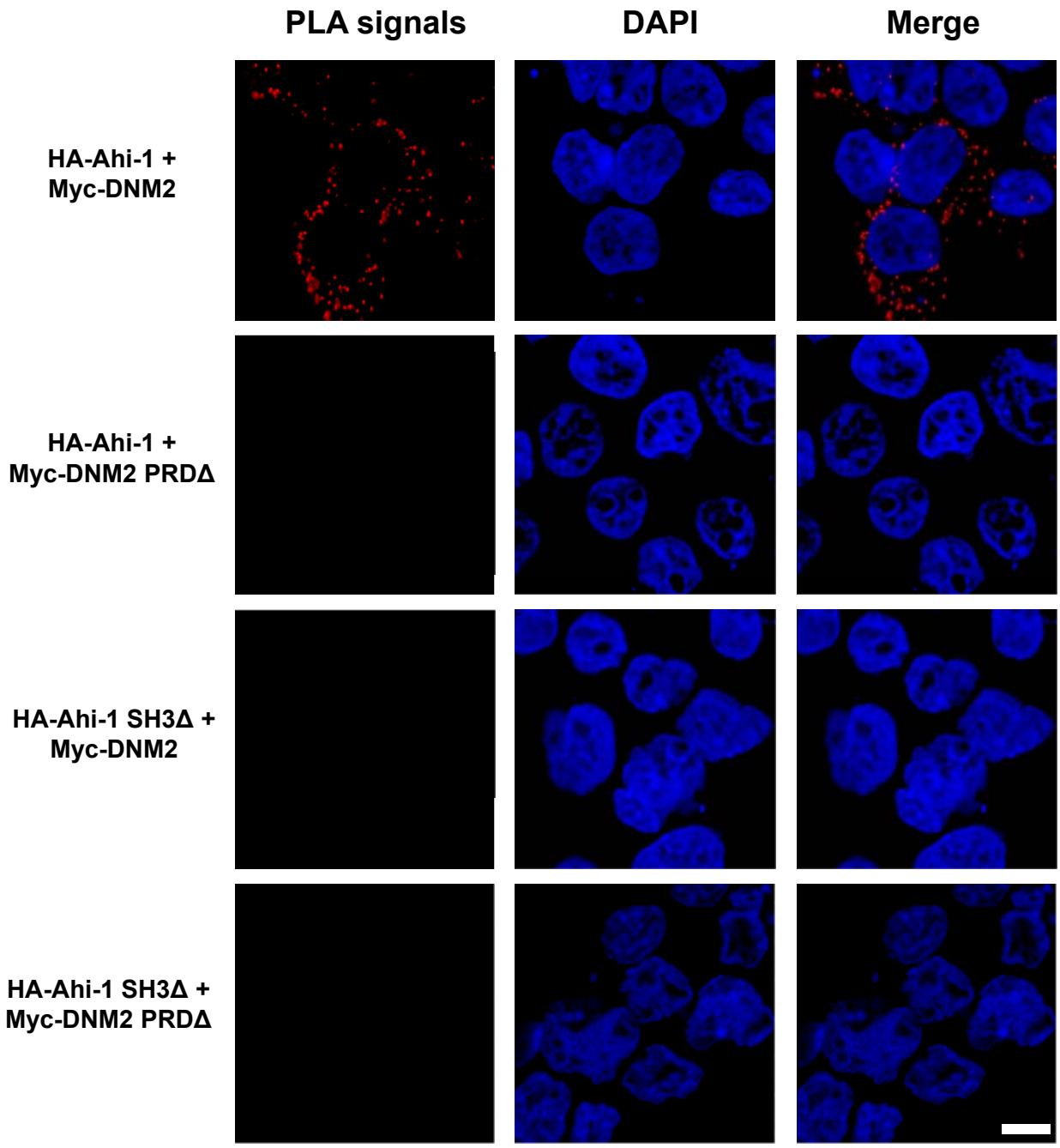

Supplementary Figure 1. The SH3 domain of Ahi-1 and the PRD of DNM2 are critical for the interaction between these two proteins. 293T cells were transfected with different combinations of HA-Ahi-1, HA-Ahi-1 SH3Δ, Myc-DNM2 and Myc-DNM2 PRDΔ as indicated. Co-transfected cells were then fixed, permeabilized, blocked and incubated with anti-HA and anti-Myc antibodies overnight, followed by addition of a PLA (proximity ligation assay) probe, ligation-ligase and amplification-polymerase solutions to detect interacting proteins. DAPI was used to stain the nuclei. Images were acquired using a confocal Nikon X1 microscope at a magnification of 60X. The white scale bar represents 5μm.

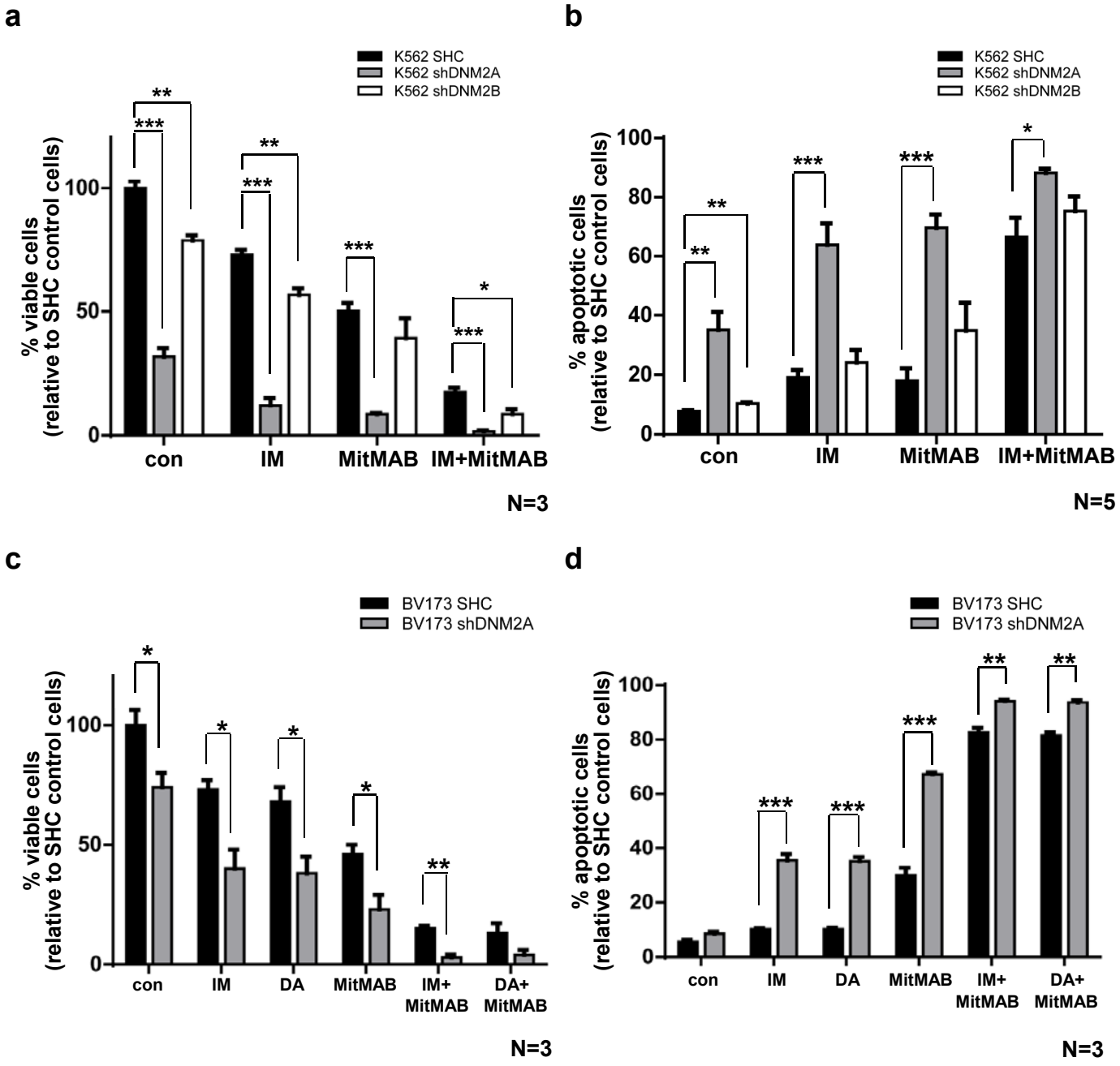

Supplementary Figure 2. Lentiviral-mediated knockdown of DNM2 in BCR-ABL$^+$ cells affects survival and apoptosis of K562 and BV173 cells. (a) Cell viability (b) and apoptosis assays in control SHC or DNM2-knockdown K562 cells treated with IM or MitMAB alone or in combination for 48 hours. (c) Cell viability (d) and apoptosis assays in control SHC or DNM2-knockdown BV173 cells treated with IM, DA or MitMAB alone or in combination for 48 hours. Values shown are the mean ± SEM. * = $p<0.05$, ** = $p<0.01$, *** = $p<0.001$.

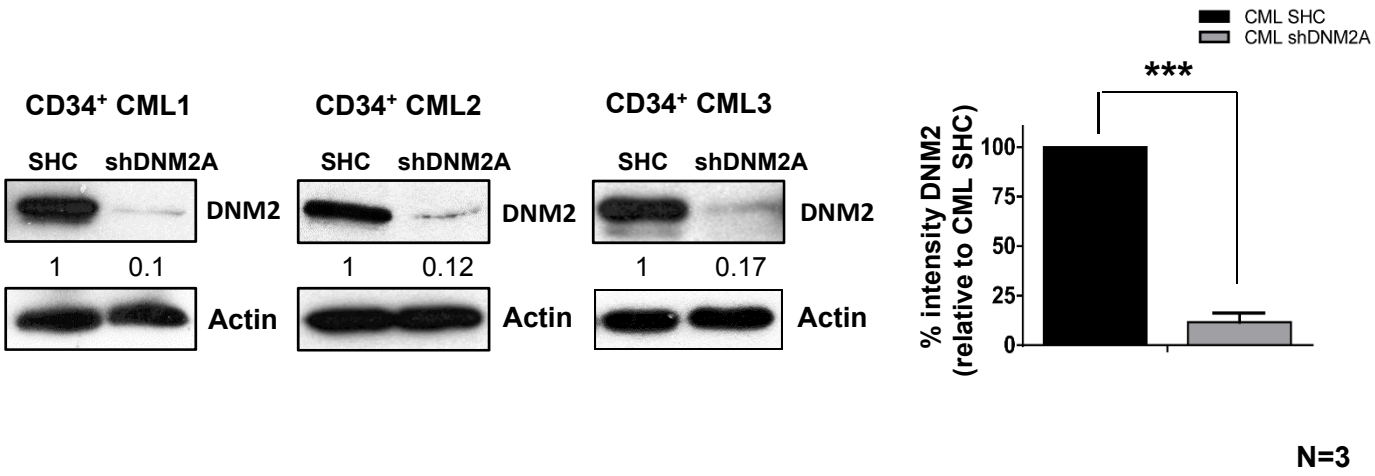

Supplementary Figure 3. DNM2 suppression in CD34$^+$ primary CML cells. Western blot analysis of CD34$^+$ CML cells from three IM-nonresponder samples transduced with either a control (SHC) or a construct containing a shRNA sequence against human DNM2 (shDNM2A, left), and quantification of suppression of DNM2 protein levels in these patient samples (right). The densitometry values of protein expression are also indicated compared to SHC control.

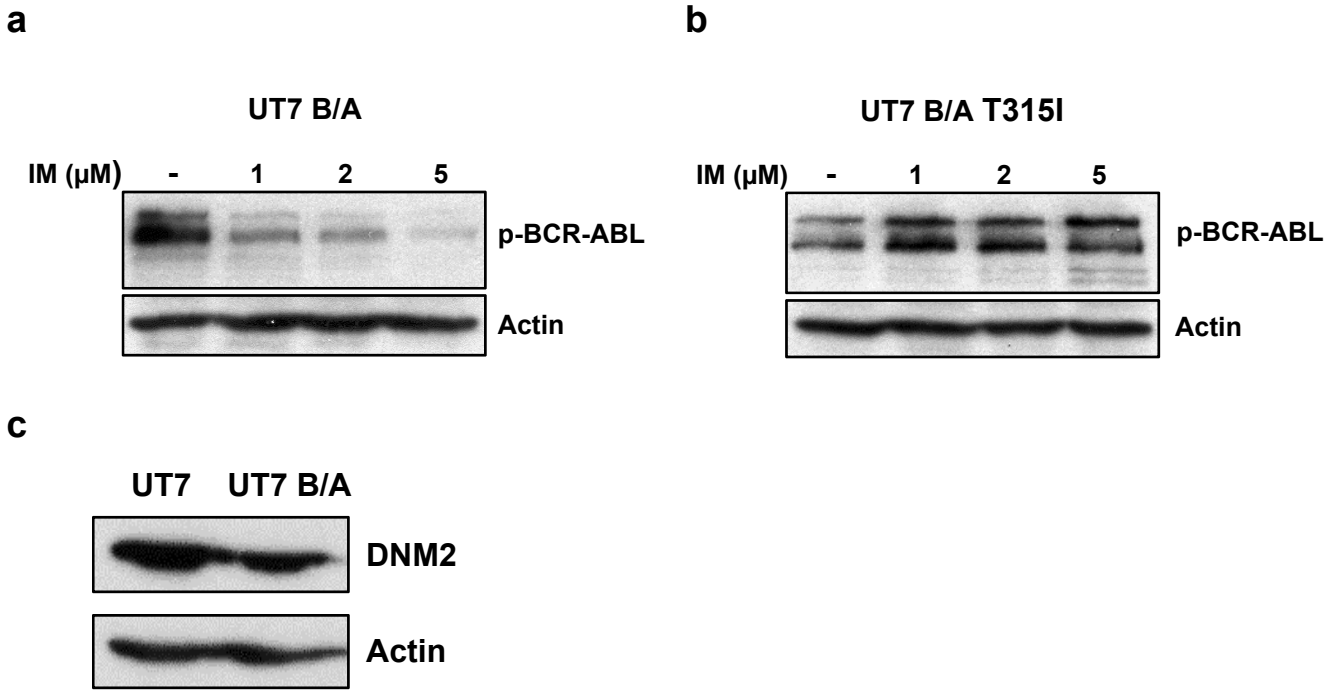

Supplementary Figure 4. Western blot analysis of BCR-ABL phosphorylation in BCR-ABL-transduced UT7 cells (UT7 B/A) and BCR-ABL-T315I mutant cells (UT7 B/A T315I) upon IM treatment. (a) + (b) Western blot analysis of BCR-ABL phosphorylation in UT7 B/A and UT7 B/A T315I mutant cells upon IM treatment with indicated doses for 24 hours. (c) Western blot analysis of DNM2 protein expression in UT7 and UT7 B/A cells. UT7 cells were cultured with human IL-3 (20ng) and GM-CSF (20ng) but not BCR-ABL-transduced UT7 cells.

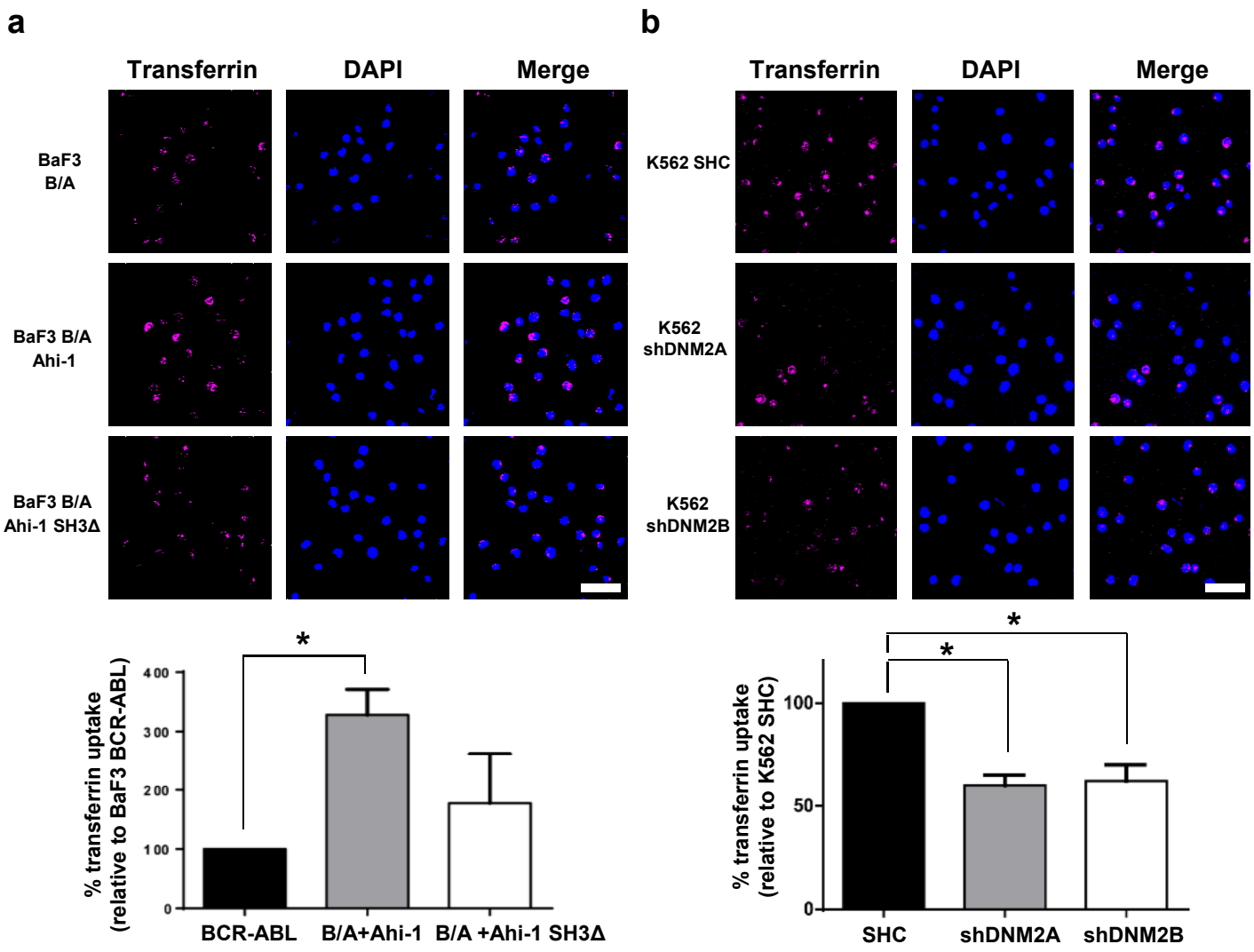

Supplementary Figure 5. Overexpression of Ahi-1 or depletion of DNM2 affects transferrin uptake in BCR-ABL$^+$ cells. (a) BCR-ABL-transduced, BCR-ABL/Ahi-1 co-transduced, BCR-ABL/Ahi-1 SH3Δ co-transduced BaF3 cells, or (b) SHC control and DNM2-knockdown K562 cells transduced with two shDNM2 constructs, were stained with Alexa Fluor 647-conjugated transferrin and transferrin uptake was determined by confocal microscopy. Representative images are shown. Intracellular transferrin signals were quantified and normalized to the signals detected in either BCR-ABL-transduced BaF3 or SHC control cells (n=3 per group). The white scale bar represents 50μm. Values shown are the mean ± SEM. * = $p<0.05$.

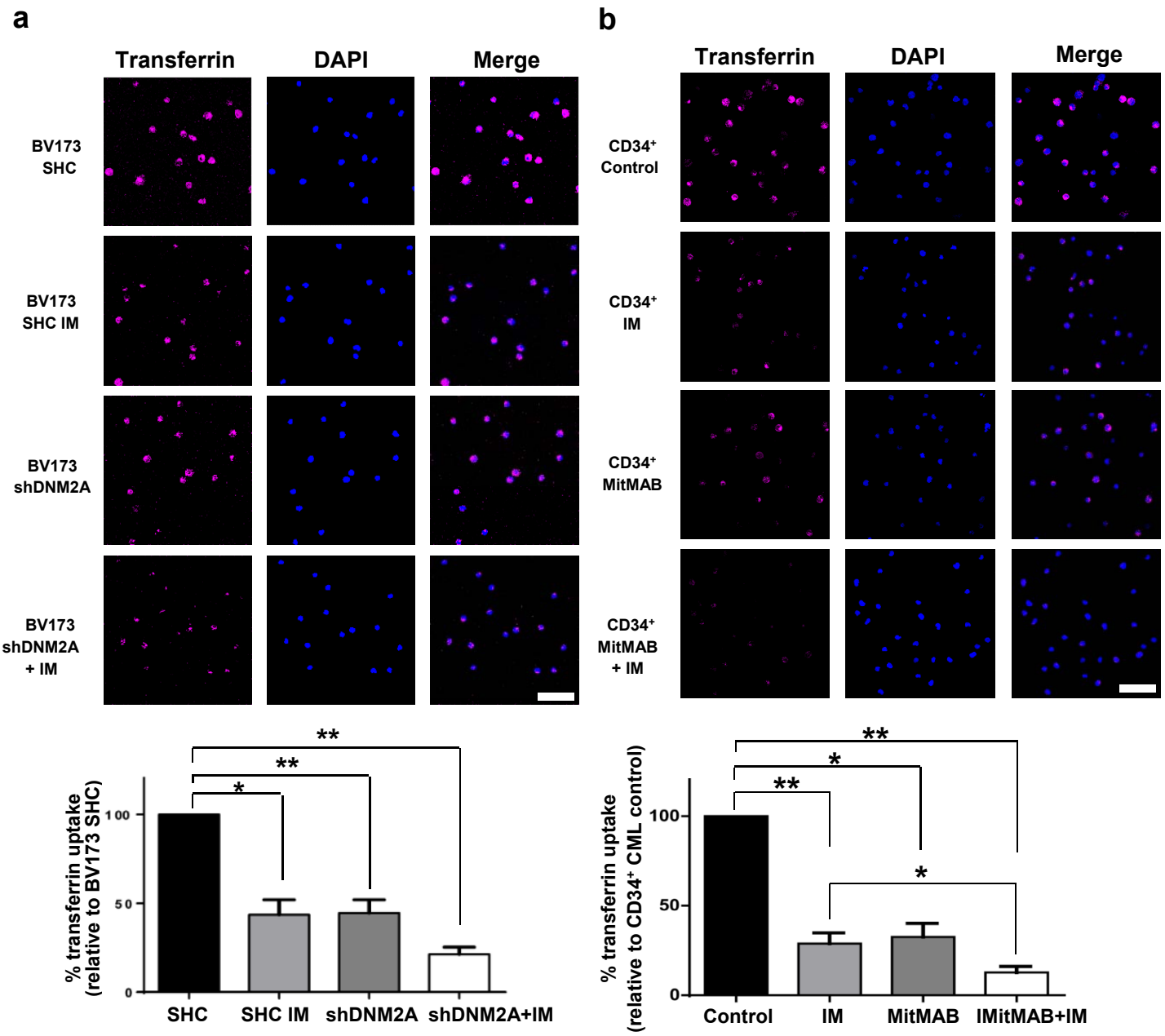

Supplementary Figure 6. Inhibition of DNM2 or BCR-ABL reduces transferrin uptake in BV173 and primary CD34⁺ CML cells from IM-responders (n=3). (a) SHC control and DNM2-knockdown BV173 cells were treated with or without 1 μM IM and (b) CD34⁺ CML cells from IM-responders were treated with or without 2.5μM MitMAB, 5μM IM or IM+MitMAB for 24 hours. Cells were stained with Alexa Fluor 647-conjugated transferrin to determine transferrin uptake by confocal microscopy. Representative images are shown. Intracellular transferrin signals were quantified for all samples and normalized to the signals detected in control cells (n=3 per group). The white scale bar represents 50μm. Values shown are the mean ± SEM. * = $p<0.05$, ** = $p<0.01$.

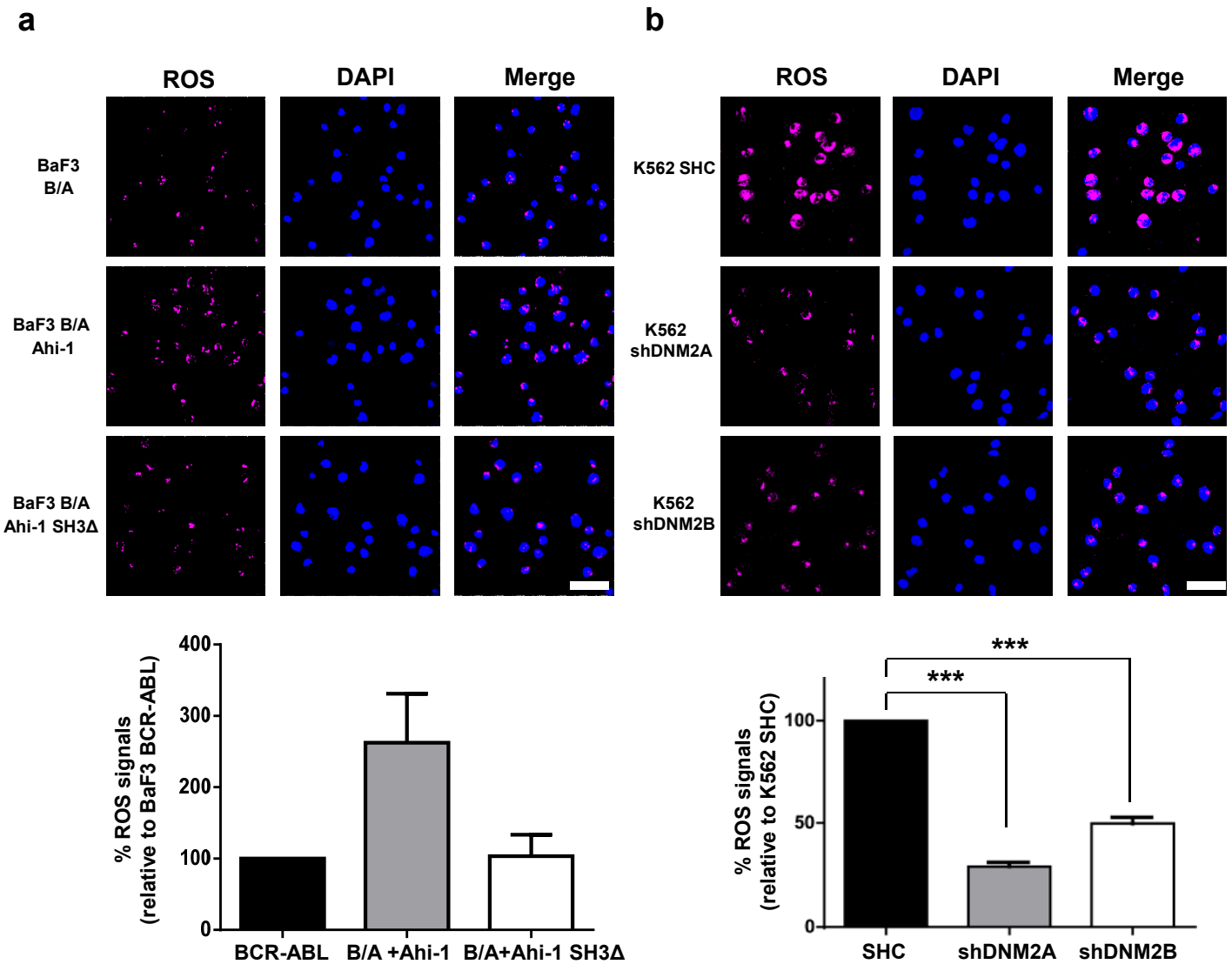

Supplementary Figure 7. Overexpression of Ahi-1 or depletion of DNM2 affects ROS production in BCR-ABL$^+$ cells. (a) BCR-ABL-transduced, BCR-ABL/Ahi-1 co-transduced or BCR-ABL/Ahi-1 SH3Δ co-transduced BaF3 cells and (b) SHC control and DNM2-knockdown K562 cells transduced with two different shDNM2 constructs were stained with CellROX deep red reagent and ROS production was determined by confocal microscopy. Representative images are shown. Intracellular ROS signals were quantified and normalized to the signals detected in either BCR-ABL-transduced BaF3 or SHC control cells (n=3 per group). The white scale bar represents 50μm. Values shown are the mean ± SEM. *** = $p<0.001$.

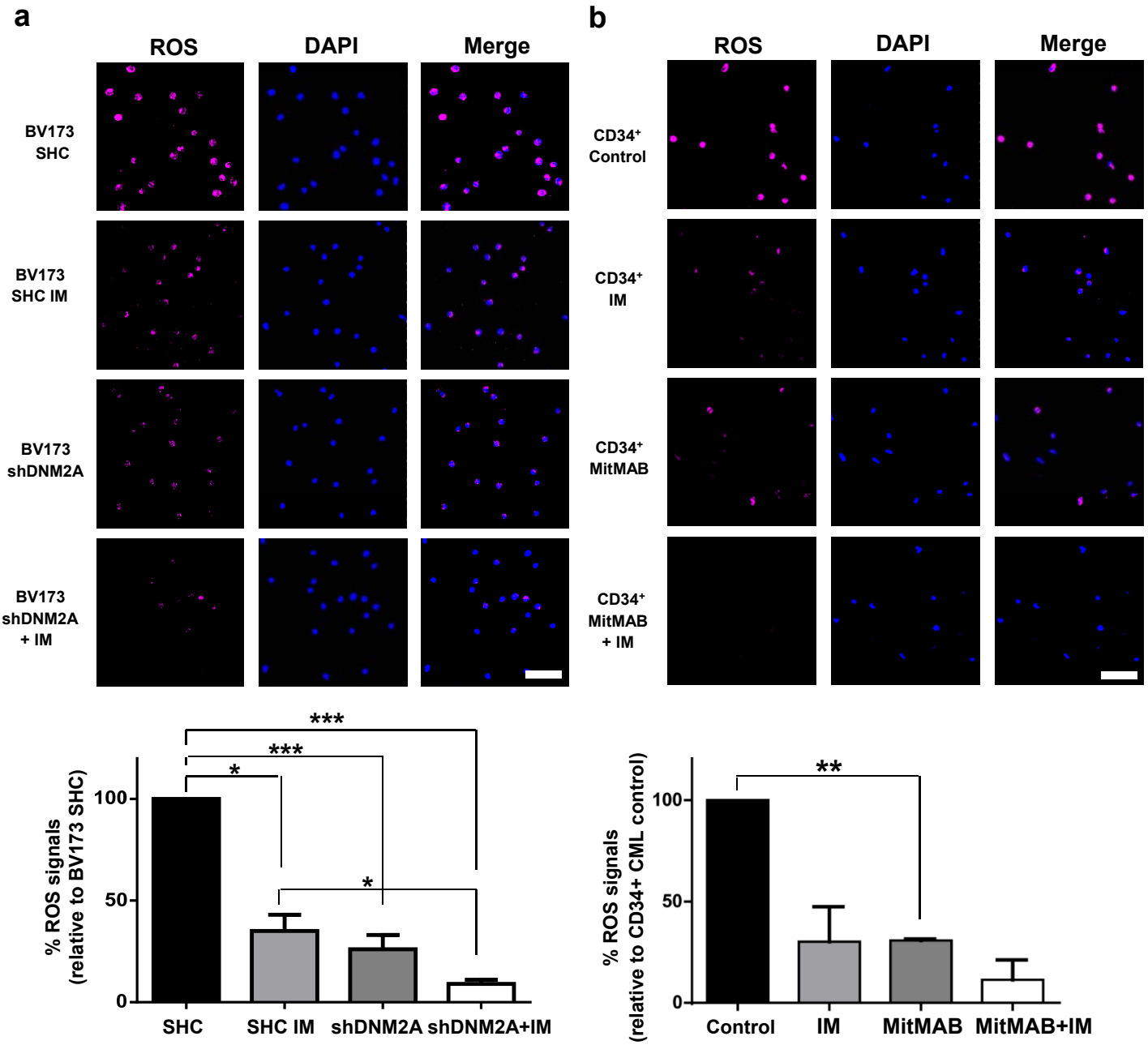

Supplementary Figure 8. Inhibition of DNM2 or BCR-ABL reduces ROS production in BV173 and primary CD34⁺ CML cells. (a) SHC control and DNM2-knockdown BV173 cells were treated with or without 1 μM IM (b) and CD34⁺ CML cells from IM-responders were treated with or without 2.5μM MitMAB, 5μM IM or IM+MitMAB for 24 hours, and stained with CellROX deep red reagent to determine ROS production by confocal microscopy. Representative images are shown. Intracellular ROS signals were quantified and normalized to the signals detected in control cells (n=3 per group). The white scale bar represents 50μm. Values shown are the mean ± SEM. * = $p<0.05$, ** = $p<0.01$.

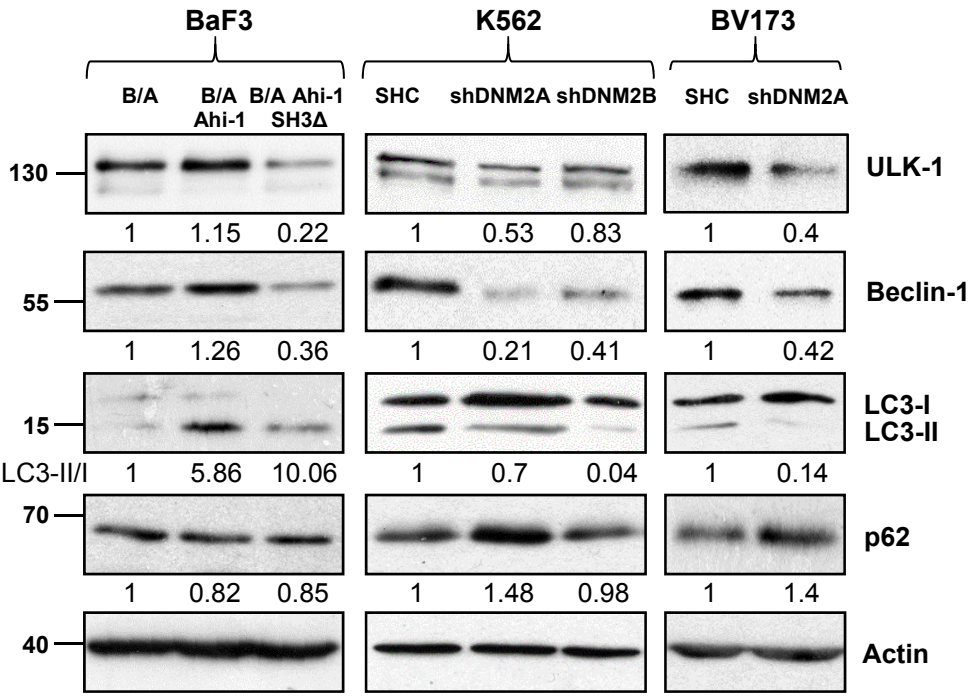

Supplementary Figure 9. Overexpression of Ahi-1 or depletion of DNM2 affects key autophagy regulators in BCR-ABL$^+$ cells. Western blot analysis of ULK-1, Beclin-1, LC3-I and LC3-II, and p62 in various BCR-ABL$^+$ cell lines with overexpression of Ahi-1 or knockdown of DNM2 as indicated. The densitometry values of protein expression compared to BCR-ABL control or SHC controls are also indicated.

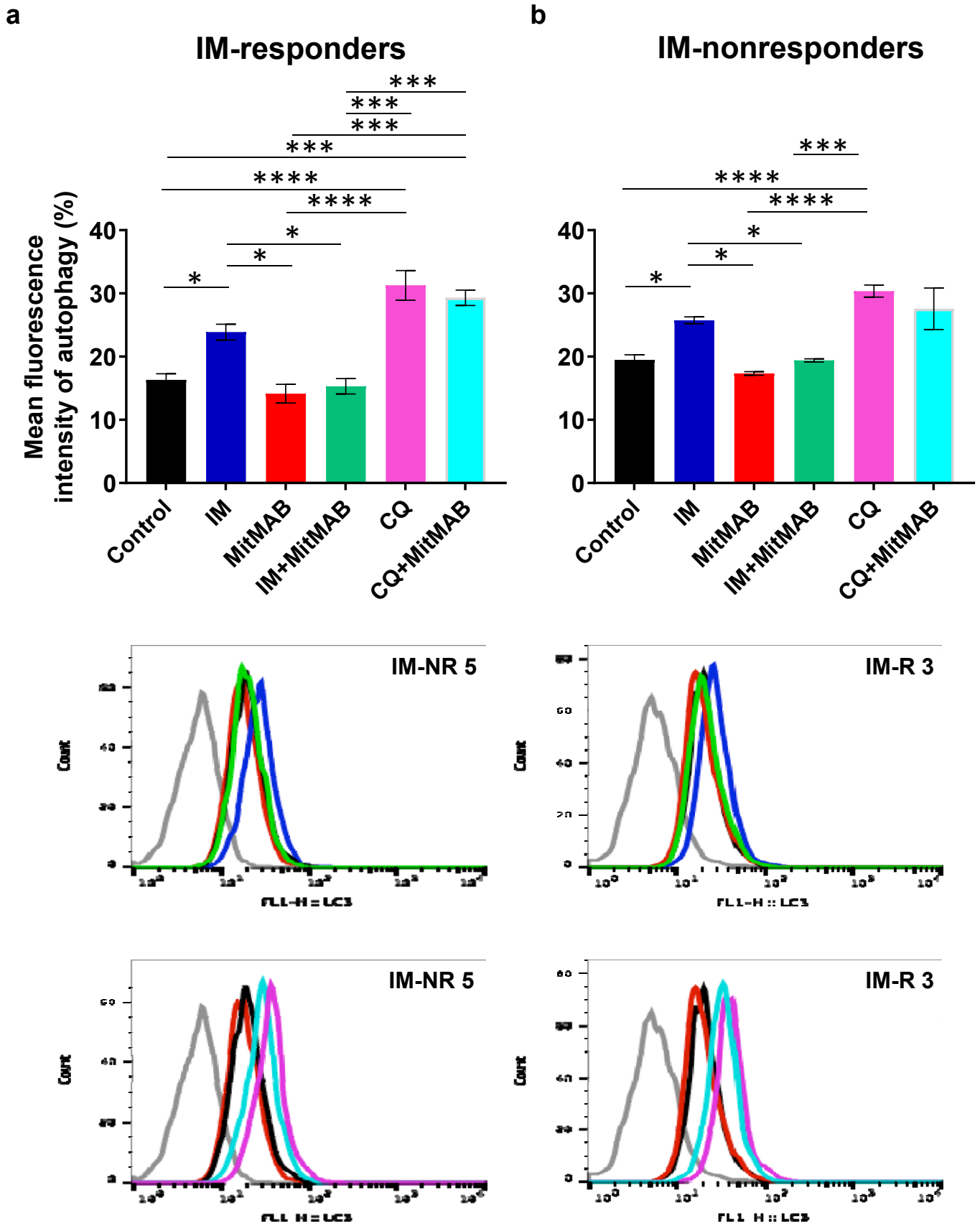

Supplementary Figure 10. Pharmacological inhibition of DNM2 reduces autophagic flux in primary CD34⁺ CML cells. (a) CD34⁺ CML cells from IM-responders or (b) IM-nonresponders were treated with 2.5μM MitMAB, 5μM IM, 20μM chloroquine (CQ), or combinations as indicated, and autophagy measured with a Cyto-ID green detection dye. Values shown in top panels are the mean ± SEM from all three samples in each group (n=3 per group). Bottom panels are representative histograms. * = p<0.05, ** = p<0.01, *** = p<0.001, **** = p<0.0001.